

# A new interpretation for the degradation phenomenon of ZnO varistors

E. R. LEITE

*Departamento Prod. Elétricos, 3M do Brasil, Via Anhanguera, Km 110, Campinas, SP Brazil*

J. A. VARELA

*Instituto de Química, UNESP, CP 355, 14800 Araraquara, SP Brazil*

E. LONGO

*Departamento de Química, UFSCar, CP 676, 13560 São Carlos, SP Brazil*

The electrical degradation phenomena of zinc oxide-based varistors were studied using a high-energy current pulse and a.c. polarization at different temperatures. Activation energy measurements during the degradation process showed that these phenomena are associated with diffusion and that the diffusion-controlling species are slower than  $Zn_i$ . For degradation promoted by current pulses of  $8 \times 20 \mu s$ , the Schottky potential barrier deformation was measured. A decrease in height and width of the potential barrier due to the reduction of surface states density,  $N_s$ , without a significant change in donor density,  $N_d$ , was observed. To explain these results, a modification of the unstable components model is proposed for the potential barrier in which the degradation is due to oxireduction reactions between atomic defects. These reactions promote the elimination of zinc vacancies and/or adsorbed oxygen on the grain boundaries.

## 1. Introduction

ZnO varistor ceramics are semiconductor devices which present high non-linearity between current density and electric field, and they are indicated for transient voltage suppression. These characteristics are essential in the use of these devices as surge arresters in substitution for traditional SiC varistors. However, a limitation of ZnO varistor is the increase in leakage current with time when a direct or pulsed current is applied [1, 2]. Several models have been proposed to explain these degradation phenomena [1–6], but the cation migration model and the unstable components model for the potential barrier seem to be the most consistent [1, 3, 4]. However, these models do not explain some characteristics of degradation phenomena with mass loss, like oxygen [5], and the lower degradation of varistors devices in oxygen atmospheres [6]. In this work the degradation phenomena of ZnO-based varistors were analysed when submitted to a.c. polarization or high-intensity current pulses. Based in the unstable components model for the potential barrier proposed by Gupta and Carlson [3] and in oxireduction reactions between atomic defects, a new model is proposed to explain the degradation phenomena in zinc oxide-based varistors.

## 2. Experimental procedure

The ZnO varistors used in this study were processed through the mixture of oxides, dry pressing and

sintering in an electrical furnace. The varistor composition was 97% ZnO, 0.5%  $Bi_2O_3$ , 1.0%  $Sb_2O_3$ , 0.5%  $Co_2O_3$ , 0.5%  $Cr_2O_3$  and 0.5%  $MnO_2$  (mol %), and the sintering temperature was 1250 °C with a 1 h soaking time.

To study the degradation by a.c. polarization, the leakage current was measured as function of time at several temperatures. The leakage current was measured in an a.c. at a fixed electric field corresponding to 85%  $E_{0.05}$ , where  $E_{0.05}$  is the electric field corresponding to a current density of 0.05 mA cm<sup>-2</sup>. This electric field was chosen because this value is located in the region where the electric conductivity is controlled by grain boundaries. The variation of leakage current with time can be described by [1]

$$I_1 - I_0 = Kt^n \quad (1)$$

where  $I_1$  is the leakage current,  $I_0$  is the initial leakage current,  $K$  is a constant related to temperature,  $t$  is the time and  $n$  is the exponent that varies from 0.3–0.9 according to the electric field polarization. For the range of electric field used in this study,  $n$  is of the order of 0.5.

For the degradation promoted by a high-intensity current pulse a 50 kJ Haefely pulse generator model E was used, for waves of  $8 \times 20 \mu s$ . The degradation was analysed from the variation of  $E_{0.05}$  as function of the number of applied pulses and from the deformation of the potential barrier, measurement of the variation of height,  $\phi$ , and the width,  $\omega$ , of the barrier, before and after the application of four cycles of 250 A cm<sup>-2</sup>, and

500 A cm<sup>-2</sup> of 8 × 20 μs waves. Each cycle consisted in the application of five current pulses and sufficient time was allowed between cycles to allow the sample to cool down to room temperature. To determine φ and ω the following points were considered:

(a) the potential barriers are of Schottky type, separated by a thin film [7];

(b) the conduction mechanism is by thermionic emission [7].

Using this hypothesis, the current density,  $J$ , is related to the electric field,  $E$ , by

$$J = J_0 \exp \frac{-(\phi - \beta E^{1/2})}{kT}, \quad (2)$$

where  $J_0$  is a constant,  $k$  is the Boltzmann constant,  $\beta$  is a constant related to the potential barrier width,  $\omega$ , and  $T$  is the absolute temperature (K). The constant  $\beta$  is given by

$$\beta = \left[ \left( \frac{1}{n\omega} \right) \left( \frac{2e^3}{4\pi\epsilon_0\epsilon_r} \right) \right]^{1/2} \quad (3)$$

where  $n$  is the number of grains in series,  $e$  is the electron charge,  $\epsilon_0$  and  $\epsilon_r$  are the vacuum and material dielectric permittivities, respectively.  $n$  is defined by

$$n = \frac{L}{G} \quad (4)$$

where  $L$  is the sample height and  $G$  is the mean grain size of ZnO determined from the scanning electron micrographs. The value of  $G$  determined in the ZnO varistor was  $13 \pm 4 \mu\text{m}$ . An energy dispersive spectrometer (EDS) attached to the SEM was used to determine the distribution of dopants in processed varistors. By plotting  $\ln J$  versus  $E^{1/2}$  (Equation 2), a straight line is obtained whose slope gives  $\beta/kT$ . The slope of the  $\ln J$  versus  $1/T$  plot gives  $(\phi - \beta E^{1/2})/k$ . Using values of  $\beta$  it is possible to calculate the barrier height,  $\phi$ . The values of  $\phi$  and  $\omega$  were determined in d.c. for different temperatures.

### 3. Results and discussion

#### 3.1. Degradation in a.c. polarization

Fig. 1 shows the increase of leakage current ( $I_t - I_0$ ) as a function of  $t^{1/2}$  for different temperatures. A linear behaviour is observed for temperatures of 70 and 85 °C. However, at 91 and 100 °C the linear behaviour is limited to  $I_t - I_0 = 2$  mA. For currents higher than this there is a thermal runaway, i.e. the power generated by the varistor is higher than its capability of dissipation, leading to thermal instability and consequently to varistor damage. The rate constant,  $K$ , determined from the plot of Fig. 1 is highly dependent on temperature, which is in agreement with Gupta and Carlson [1, 4].

Fig. 2 shows the Arrhenius plot for  $K$  values determined from the curves in Fig. 1. The apparent activation energy determined is  $Q = 0.96$  eV with  $K_0 = 1.5 \times 10^{13}$  mA min<sup>-1/2</sup>. This value is compared with other activation energies determined in the literature and given in Table I.

The values of 0.50 and 0.55 eV [4, 8] are related to the diffusion of  $Zn_i$  in pure ZnO; the value of 0.80 eV

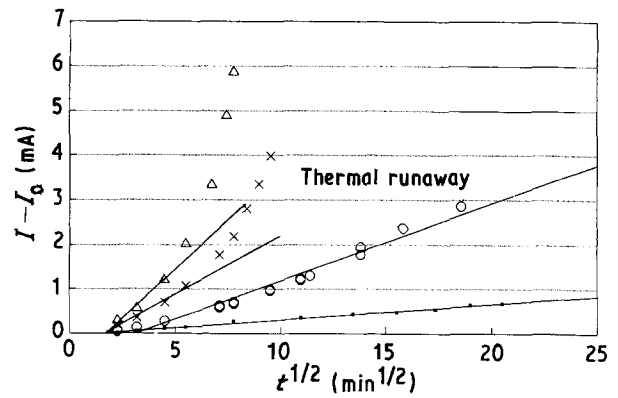
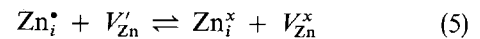


Figure 1 Increase of leakage current as a function of  $t^{1/2}$  at different temperatures: (■) 70 °C, (○) 85 °C, (×) 91 °C, (△) 100 °C.

TABLE I Comparison of values of activation energy determined during varistor degradation

$Q$ (eV)	References
0.96	Present work
0.67	[1, 4]
0.50	[4]
0.55	[8]
0.80	[5]

[5] is attributed to the desorption of oxygen from ZnO grain boundaries; and the value of 0.67 eV was associated with the process of ZnO varistor degradation [1, 4]. Gupta and Carlson associated this value (0.67 eV) with  $Zn_i$  diffusion following the reaction with  $V_{Zn}$  at grain boundaries, according to



The reaction of  $Zn_i^*$  and  $V_{Zn}'$  at grain boundaries is responsible for the reduction in potential barrier height.

The value of 0.96 eV for apparent activation energy measured in this work indicates that the degradation is not controlled by diffusion of  $Zn_i$  but by the diffusion of slower species, because the process of degradation is related to the diffusion process (see Fig. 1). According to these results it is necessary to review the unstable components of the potential barrier model [3] because this model considers only  $Zn_i$  as the diffusing component.

#### 3.2. Degradation due to current pulses

Fig. 3 shows the variation of  $E_{0.05}$  as a function of the number of 500 A cm<sup>-2</sup> (8 × 20 μs waves) pulses applied. A gradual reduction of  $E_{0.05}$  was observed, indicating an increase of leakage current.

Fig. 4 shows curves of  $\ln J$  versus  $E^{1/2}$  and  $\ln J$  versus  $1/T$  for varistors before degradation. A linear behaviour in both curves is observed, which indicates that the model used describes the conduction mechanism well for ZnO varistors. Values of potential barrier height,  $\phi$ , and barrier width,  $\omega$ , were measured before and after application of 20 current pulses (250 and 500 A cm<sup>-2</sup>) and are presented in Table II. Both

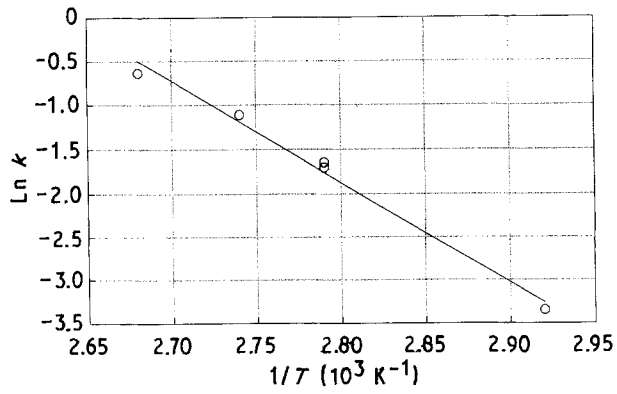


Figure 2 Arrhenius plot for ZnO varistor degradation.

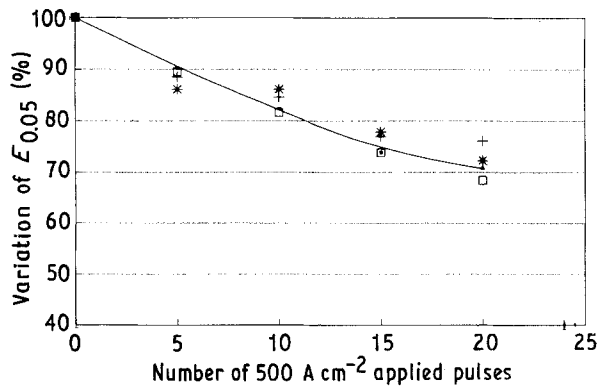


Figure 3 Variation of  $E_{0.05}$  as function of  $500 \text{ A cm}^{-2}$  current pulse number.

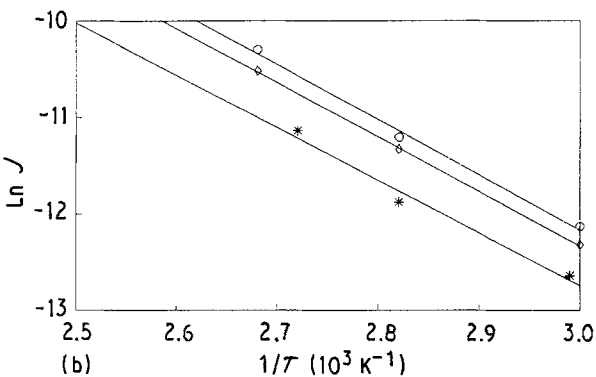
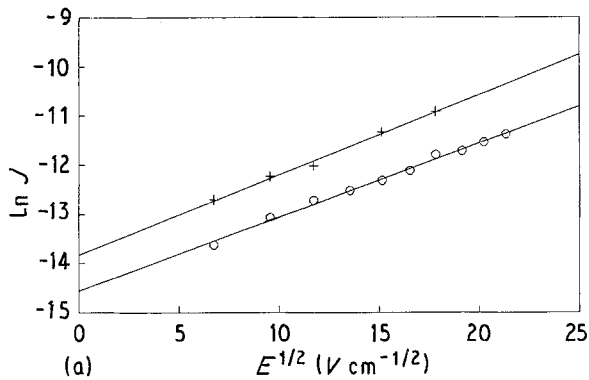


Figure 4 Log current density as function of (a)  $E^{1/2}$  at (○)  $60^\circ\text{C}$ , (+)  $80^\circ\text{C}$  for Sample 45; and (b)  $1/T$  for samples (◇) 45, (○) 1, and (\*) 9.

TABLE II Variation of  $\phi$  and  $\omega$  with applied current pulses in  $8 \times 20 \mu\text{s}$  waves measured at  $60^\circ\text{C}$

Sample	$\phi$ (eV)	$\omega$ (nm)
No applied pulses	$0.40 \pm 0.02$	$13 + 1.5$
After 20 pulses of $250 \text{ A cm}^{-2}$	$0.40 \pm 0.01$	$10.5 \pm 0.9$
After 20 pulses of $500 \text{ A cm}^{-2}$	0.34	7.9

$\phi$  and  $\omega$  decrease with applied pulses, but  $\omega$  is more sensitive to degradation than  $\phi$ .

The electric field at  $500 \text{ A cm}^{-2}$  does not change with applied pulses. This implies that the current pulses affect only the grain boundary region without modification of the ZnO bulk conductivity.

In the Schottky-type potential barrier model [9],  $\phi$  is described as

$$\phi = \frac{e^2 N_s^2}{2 \epsilon_0 \epsilon_r N_d} \quad (6)$$

where  $N_s$  is the surface states density (negative charges) and  $N_d$  is the donor density in the depletion layer (positive charges). In this model,  $\phi$  is modified by changing either  $N_s$  or  $N_d$ . Moreover,  $N_d$  is related to  $\phi$  and  $\omega$  by

$$N_d = \frac{\{2 \epsilon_0 \epsilon_r [\phi - (E_c - E_F)]\}}{e^2 \omega^2} \quad (7)$$

where  $E_c$  is the bottom energy of the conduction band and  $E_F$  is the Fermi energy. All parameters of Equation 7 are known, except  $(E_c - E_F)$ . However, this parameter in the system ZnO·CoO was measured, and its value is 0.30 eV [6]. If we consider that the main dopant in a ZnO varistor is cobalt, as shown in Fig. 5, this value can be used in this study with the hypothesis that it does not change with degradation. Then  $N_d$  was measured from Equation 7 for samples before and after degradation with 20 current pulses, as shown in Table III. It is verified from this table that  $N_d$  does not change significantly even though the Schottky barrier was deformed.

The surface state density,  $N_s$ , can be determined from

$$N_s = \frac{Q_s}{e} \quad (8)$$

where  $Q_s$  is the total trapped charge at the interface and can be described as

$$Q_s = 2 \int_0^\omega N_d e dx \quad (9)$$

Considering that  $N_d$  is independent of  $x$ , Equation 9 becomes

$$Q_s = 2 N_d e \omega \quad (10)$$

From Equations 8 and 10,  $N_s$  is related to  $N_d$  by

$$N_s = 2 \omega N_d \quad (11)$$

Equation 11 is the electrical neutrality condition for the material. As observed in Table III,  $N_d$  does not change with degradation and  $\omega$  decreases with potential barrier deformation. In this way the degradation

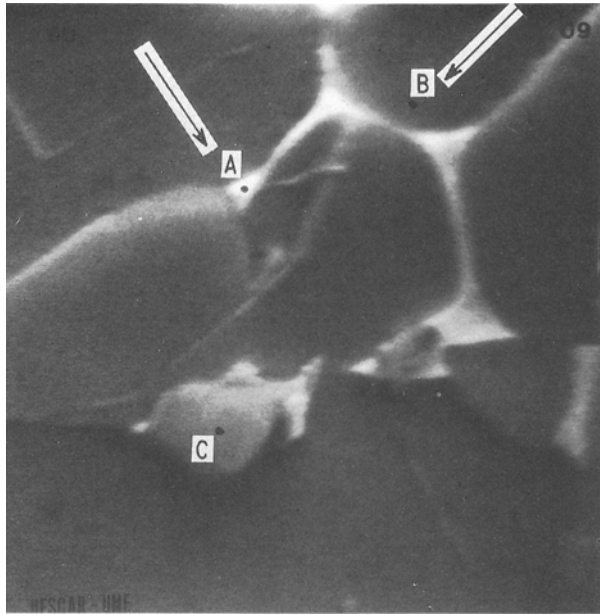


Figure 5 Microstructure of ZnO varistor (secondary electron image). Points A–C were analysed by EDS. Concentrations: A, Bi high, Zn low; B, Zn high, Co low; C, Zn high, Sb high, Co low, Mn low, Cr low.

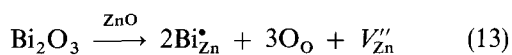
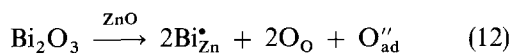
TABLE III  $N_d$  calculated from Equation 7 before and after 20 current pulses

	$N_d$ ( $\text{cm}^{-3}$ )
Before applied pulse	$0.65 \times 10^{18} (\pm 0.22)$
After 20 pulses of $250 \text{ A cm}^{-2}$	$0.76 \times 10^{18} (\pm 0.23)$
After 20 pulses of $500 \text{ A cm}^{-2}$	$0.60 \times 10^{18}$

phenomena are due to the reduction of  $N_s$ , i.e. reduction of negative charges trapped in the ZnO grain boundaries.

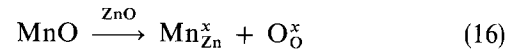
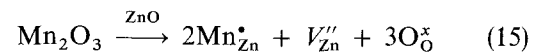
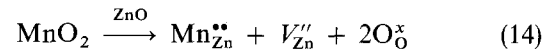
### 3.3. General discussion

The formation of a potential barrier is due to charged atomic defects [3] formed during sintering of ZnO varistors. These defects formed at a depletion layer are positive ( $\text{Zn}_i^+$ ,  $\text{Zn}_i^{2+}$ ,  $\text{V}_O^\bullet$ ,  $\text{V}_O^{\bullet\bullet}$ ,  $\text{M}_{\text{Zn}}^+$ ,  $\text{M}_{\text{Zn}}^{2+}$ , where M is a metal ion replacing zinc) and are compensated by negative charges at grain boundaries ( $\text{V}_{\text{Zn}}'$ ,  $\text{V}_{\text{Zn}}''$ ,  $\text{O}_{\text{ad}}''$ ). These potential barriers are formed during the sintering process, due to doping effects. The solid solution of  $\text{Bi}_2\text{O}_3$  in ZnO will generate the following defects

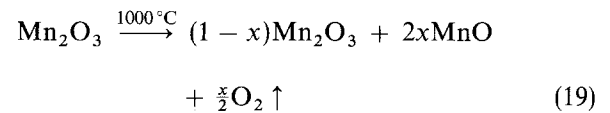
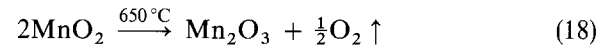


In these reactions the formation of positive charges ( $\text{Bi}_{\text{Zn}}^+$ ) and negative charges are observed, due to zinc vacancies or adsorbed oxygen. These negatively charged defects at the interface are necessary in order to compensate for the positively charged defects created at the depletion layer [10].

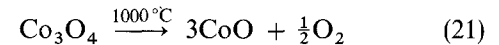
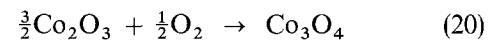
The solid solution of  $\text{MnO}_2$  in the ZnO matrix generates defects according to the following reactions



The defect reactions indicated in Equations 14–16 are due to different oxidation states of manganese. During heating of  $\text{MnO}_2$  there is a reduction of  $\text{Mn}^{4+}$  according to the following equations



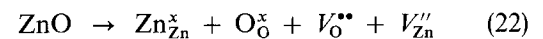
The same behaviour is expected to occur in  $\text{Co}_2\text{O}_3$ -doped ZnO. However,  $\text{Co}_2\text{O}_3$  is oxidized during heating and then reduced at temperatures above  $1000^\circ\text{C}$



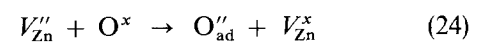
This oxidation followed by reduction may be the reason for the low influence of cobalt oxide as a dopant on the non-ohmic properties of ZnO-based varistors [11, 12].

Considering Reactions 12–17 to be responsible for the formation of a potential barrier and consequently for the non-linearity of ZnO-based varistors, the degradation should be promoted by reactions that eliminate the defects formed during sintering. Thus there is a migration of ions in the depletion layer to the interface followed by the interaction of these positive charges with the negative charges of the interface, with a consequent reduction of the surface state density,  $N_s$ .

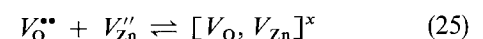
The reactions between defects proposed by Gupta and Carlson [3] consider that the unstable component at the depletion layer is  $\text{Zn}_i^+$  or  $\text{Zn}_i^{2+}$ . However, if we consider that the major concentration of ionized carriers at the depletion layer is oxygen vacancies ( $\text{V}_O^\bullet$ ,  $\text{V}_O^{\bullet\bullet}$ ), the defect reaction can be written as

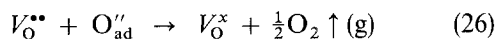


During cooling after the sintering process, oxygen can react with  $\text{V}_{\text{Zn}}''$  as follows



Then two negative components can exist at the interface, i.e. a zinc vacancy,  $\text{V}_{\text{Zn}}''$ , and adsorbed oxygen,  $\text{O}_{\text{ad}}''$  [13]. In this way the migration of  $\text{V}_O^{\bullet\bullet}$  or  $\text{V}_O^\bullet$  (possible defects on the depletion layer) to the interface leads to the following reactions





Reaction 26 explains the weight loss during the degradation phenomena of the ZnO varistor by the loss of oxygen. Moreover, this reaction can explain the lower degradation of the ZnO varistor in an oxygen atmosphere.

#### 4. Conclusions

The results of this study show that the degradation phenomena in ZnO-based varistor, measured from the leakage current, are proportional to  $t^{1/2}$ . The process is temperature dependent with an activation energy of 0.96 eV, which indicates that the process is not controlled by  $Zn_i$  diffusion but by another slow species.

The results also show that for samples degraded by high-intensity current pulses there is a reduction in  $\phi$  and  $\omega$ , with  $N_d$  remaining practically constant with reduction of  $N_s$ . This reduction in  $N_s$  is promoted by reactions between the depletion layer defects ( $V_{\text{O}}^{\bullet\bullet}$ ,  $V_{\text{O}}^{\bullet}$ ,  $Zn_i^{\bullet\bullet}$ ,  $Zn_i^{\bullet}$ ) and interface defects ( $V_{\text{Zn}}''$ ,  $V_{\text{Zn}}'$ ,  $O_{\text{ad}}''$ ,  $O_{\text{ad}}'$ ) which lead to the reduction in defect concentration formed during sintering.

In order to explain the phenomena of degradation in a ZnO-based varistor, a modification of Gupta and Carlson's [3] model is considered, in which new unstable components at the depletion layer ( $V_{\text{O}}^{\bullet}$  and  $V_{\text{O}}^{\bullet\bullet}$ ) and new interface charges ( $O_{\text{ad}}''$  and  $O_{\text{ad}}'$ ) are proposed. With these components it is possible to explain the weight loss during the ZnO varistor degradation and the lower degradation in an oxygen-rich atmosphere. Both voltage barrier formation and degradation can

be explained by an oxi-reduction reaction between atomic defects.

#### Acknowledgement

The authors thank 3 M do Brasil, FAPESP and CNPq for financial support for this project.

#### References

1. T. K. GUPTA and W. G. CARLSON, *J. Appl. Phys.* **52** (1981) 4104.
2. C. G. SHIRLEY and W. M. PAULSON, *ibid.* **50** (1979) 5782.
3. T. K. GUPTA and W. G. CARLSON, *J. Mater. Sci.* **20** (1985) 3487.
4. *Idem.*, "Additives and Interfaces in Electronic Ceramics", in "Advances in Ceramics", Vol. 7, edited by F. M. Yan and H. H. Heuer (American Ceramic Society, Columbus, Ohio, 1983) p. 30.
5. D. BINESTI, PhD thesis, University of Bordeaux I, Bordeaux, France (1985).
6. H. R. PHILIPP and L. M. LEVINSON, in "Additives and Interfaces in Electronics Ceramics, Advances in Ceramics", Vol. 7, edited by M. F. Yam and H. H. Heuer (American Ceramic Society, Columbus, Ohio, 1983) p. 1.
7. K. EDA, *J. Appl. Phys.* **49** (1978) 2964.
8. R. A. SWALIN, "Thermodynamics of Solids" (Wiley, New York, 1964).
9. W. HEYWANG, *J. Amer. Ceram. Soc.* **47** (1964) 484.
10. B. TANOUTI, PhD thesis, University of Bordeaux I, Bordeaux, France (1985).
11. S. A. PIANARO, Ms thesis, UFSCar, São Carlos (1990).
12. A. SMITH, J. F. BAUNARD, P. ABETARD and M. F. DENAROT, *J. Appl. Phys.* **65** (1989) 5119.
13. S. FUJITSU, K. KOUMOTO and H. YANAGIDA, *Solid State Ionics* **32/33** (1989) 482.

Received 17 June  
and accepted 16 December 1991